NASA Technical Memorandum 4705

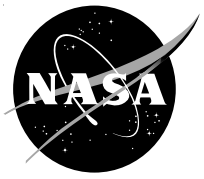

Flight Assessment of the Onboard Propulsion System Model for the Performance Seeking Control Algorithm on an F-15 Aircraft

John S. Orme and Gerard S. Schkolnik

July 1995

Flight Assessment of the Onboard Propulsion System Model for the Performance Seeking Control Algorithm on an F-15 Aircraft

John S. Orme
Gerard S. Schkolnik
NASA Dryden Flight Research Center
Edwards, California

Technical Memorandum 4705 July 1995

FLIGHT ASSESSMENT OF THE ONBOARD PROPULSION SYSTEM MODEL FOR THE PERFORMANCE SEEKING CONTROL ALGORITHM ON AN F-15 AIRCRAFT

John S. Orme* and Gerard S. Schkolnik†
NASA Dryden Flight Research Center
Edwards, California

Abstract

Performance Seeking Control (PSC), an onboard, adaptive, real-time optimization algorithm, relies upon an onboard propulsion system model. Flight results illustrated propulsion system performance improvements as calculated by the model. These improvements were subject to uncertainty arising from modeling error. Thus to quantify uncertainty in the PSC performance improvements, modeling accuracy must be assessed. A flight test approach to verify PSC-predicted increases in thrust (*FNP*) and absolute levels of fan stall margin is developed and applied to flight test data. Application of the excess thrust technique shows that increases of *FNP* agree to within 3 percent of full-scale measurements for most conditions. Accuracy to these levels is significant because uncertainty bands may now be applied to the performance improvements provided by PSC. Assessment of PSC fan stall margin modeling accuracy was completed with analysis of in-flight stall tests. Results indicate that the model overestimates the stall margin by between 5 to 10 percent. Because PSC achieves performance gains by using available stall margin, this overestimation may represent performance improvements to be recovered with increased modeling accuracy. Assessment of thrust and stall margin modeling accuracy provides a critical piece for a comprehensive understanding of PSC's capabilities and limitations.

Acronyms

ADECS	Advanced Engine Control System
AEDC	Arnold Engineering Development Center, Tullahoma, Tennessee
CDP	Component Deviation Parameters
CPSM	Compact Propulsion System Model
DEEC	Digital Electronic Engine Control
DEFCS	Digital Electronic Flight Control System
DFRC	Dryden Flight Research Center, Edwards, California
HIDEC	Highly Integrated Digital Electronic Control
Kf	Kalman filter
MDA	McDonnell Douglas Aerospace, St. Louis, Missouri
OFP	Operational Flight Program
PSC	Performance Seeking Control
PW	Pratt & Whitney, West Palm Beach, Florida
S/MTD	STOL Maneuver Technology Demostrator
TTW	total temperature and weight flow method
VMSC	Vehicle Management System Computer

Nomenclature

A_J	nozzle throat area, in^2
C_{Decs}	environmental control system bleed air drag
C_{Dpb}	plenum bleed drag

*Aerospace Engineer. Member AIAA.
†Aerospace Engineer. Member AIAA.

C_{Dtrim}	combined inlet spillage and trim drag
CIVV	compressor inlet variable guide vane angle, deg
D	total aircraft drag, lb
D_{INL}	incremental inlet spillage drag, lb
D_{NOZ}	nozzle drag, lb
D_{STAB}	incremental stabilator and inlet cowl trim drag, lb
EPR	engine pressure ratio, P_{T6}/P_{T2}
F_{ex}	excess thrust, lb
F_G	gross thrust, lb
F_N	net thrust, lb
FNP	net propulsive force, lb
FPR	fan pressure ratio, $P_{T2.5}/P_{T2}$
FPR_{CIVV}	off schedule *CIVV* factor
FPR_{dis}	inlet distortion factor
FPR_i	installed stall line *FPR*
FPR_o	operating *FPR*
FPR_{Re}	Reynolds factor
F_R	ram drag, lb
H	pressure altitude, ft
M	Mach
N_1	fan rotor speed, rpm
N_{1C2}	fan rotor speed, corrected to station 2, rpm
N_2	compressor rotor speed, rpm
N_x	longitudinal acceleration, *g*
PD	percent difference, percent
PLA	power lever angle, deg
P_{S2}	static pressure at engine face, psi
P_T	total pressure, psi
RCVV	rear compressor variable vanes, deg
SMF	fan stall margin
SMHC	high-pressure compressor stall margin
SSVM	steady-state variable model
SVM	state variable model
TSFC	thrust specific fuel consumption, sec^{-1}
T_T	total temperature, °R
V_T	true airspeed, kn
WACC	DEEC-calculated corrected fan airflow, lb/sec
W_{Cfan}	corrected fan airflow, lb/sec
W_{Chpc}	corrected high pressure compressor airflow, lb/sec
WF	gas generator fuel flow, lb/hr
$WF_{A/B}$	afterburner fuel flow, lb/hr
W_{fan}	fan airflow, lb/sec
Wt	aircraft weight, lb
Wt_0	zero fuel aircraft weight, lb
Wt_f	total indicated fuel weight, lb
α	angle of attack, deg
β	angle of sideslip, deg
ρ	inlet cowl angle, deg
Δ_3	inlet third ramp angle, deg
η	random effects

Subscripts

meas	measured value
model	modeled value

Superscript

'	postflight model-predicted value

Prefix

Δ	perturbation or difference

Suffix, PW1128 Engine Station Numbers (fig. 2)

2	fan inlet or engine face
2.5	compressor inlet
3	compressor discharge
4	combustor exit
4.5	low-pressure turbine inlet
6	augmentor inlet
7	exhaust nozzle throat

Introduction

Optimizing the integrated control variables is an important way to improve the performance of an airplane. For example, the Advanced Engine Control System (ADECS), flight tested by NASA in the early 1980's, was the first to use digitally communicated information between the flight control and engine control computers to increase engine performance.[1] A shortcoming of the ADECS design was that it was based on predetermined control schedules. This shortcoming made the system unable to distinguish and optimize for unique operating characteristics between different engines of the same class (for example, two F100 engines with different levels of degradation).

Recently, an advanced optimization routine, called Performance Seeking Control (PSC), was flown onboard a NASA F-15 aircraft.[2] The PSC is a model-based, real-time adaptive, onboard propulsion system optimization algorithm with in-flight thrust calculation capability. The PSC method of in-flight thrust determination closely resembles the total temperature and weight flow (TTW) method first developed during the XB-70 flight test program.[3] Limited assessment of PSC modeling accuracy has been reported for calculated internal engine temperatures, pressures, and rotor speeds as well as for static thrust stand measurements.[4–6] Accuracy of the PSC in-flight *FNP* calculation needs to be assessed to evaluate the future value of the PSC concept.

The PSC performance improvements[6–10] derived from reducing stability margins are based on model calculations that may be in error by an unknown amount. During flight test of the PSC algorithm, engine performance was improved by reducing the calculated fan stall margin (SMF), thus operating closer to the predicted surge line. Accuracy of the PSC SMF model needs to be assessed.

Flight test techniques and analysis were designed by NASA Dryden Flight Research Center (DFRC) to assess the PSC modeling accuracy of net propulsive force (*FNP*) and SMF. A methodology similar to the "accelerometer method" derived by Beeler, et al.,[11] and applied by Ray for evaluating thrust calculation methods during throttle transients[12] was adopted for analysis of quasi-steady state *FNP* estimations during level accelerations. Accuracy of modeled increases in *FNP* was determined by comparisons with measured increases of excess thrust. The PSC stall margin modeling was assessed by intentionally stalling the fan in-flight and analyzing the SMF estimate. At the point the fan stalls, the estimate should be zero.

This paper describes the results of an independent assessment of the PSC thrust calculation and SMF model accuracy. Flight tests were flown from Mach 0.5 to Mach 2.0 at intermediate and maximum afterburning power settings.

Aircraft and Engine Description

The PSC algorithm has been tested on the twin-engine, high-performance McDonnell Douglas Aerospace (St. Louis, Missouri) (MDA) F-15 airplane (fig. 1). The DFRC modified the F-15 airplane to the Highly Integrated Digital Electronic Control (HIDEC) for the purpose of integrated control research. Unique HIDEC features include a digital electronic flight control system (DEFCS), two Pratt & Whitney (PW) (West Palm Beach, Florida) F100-PW-1128 engines with digital controls, and the digital data buses.

EC90 312-3

Fig. 1. The F-15 highly integrated digital electronic control aircraft.

Additional information on the F-15 airplane can be found in ref. 1.

Figure 2 shows the F100-PW-1128 engine. This low-bypass ratio, twin-spool, afterburning turbofan engine is a derivative of the F100-PW-100 engine. The engine is controlled by a full-authority digital electronic engine control (DEEC) that is similar to the current production F100-PW-220 engine controller. The DEEC provides open-loop scheduling and closed-loop feedback control of corrected fan speed (N_{1C2}) and engine pressure ratio (*EPR*) by way of the fuel flow (*WF*) and the nozzle area (A_J). The compressor inlet variable guide vane (*CIVV*) and rear compressor variable vane (*RCVV*) positions are scheduled with rotor speeds using open-loop control. The DEEC software has been modified to accommodate PSC trim commands; however, the normal DEEC control loops, such as N_{1C2} and *EPR*, have not been modified. Reference 13 gives a more detailed description of the PW1128 engine.

Performance Seeking Control Algorithm

The PSC as developed by MDA and PW and installed on the NASA F-15 HIDEC aircraft is a model-based, adaptive algorithm which performs real-time optimization of the propulsion system during quasi-steady-state operation. Information available from the onboard airdata, flight control, and engine control digital computers is shared with the PSC software. Essentially, the algorithm consists of an estimation routine to update propulsion models and an optimization routine to optimize the controlled variables.

The PSC algorithm and software was hosted on a Vehicle Management System Computer (VMSC). Figure 3 summarizes implementation of the PSC algorithm into the HIDEC aircraft. The three major algorithm elements as they reside in the VMSC consist of the identification, modeling, and optimization components. Four optimization modes were used during the flight testing. They are the (1) maximum thrust mode for enhanced aircraft acceleration, (2) minimum fuel mode for improved fuel efficiency during cruise, (3) minimum turbine temperature mode for extending engine life during cruise, and (4) rapid deceleration mode for reductions in time to decelerate from supersonic to subsonic conditions. Each of these modes produced beneficial performance improvements,[6–10] but all the accrued benefits equally rely upon on accurate in-flight thrust calculation. Modes 1 and 4 seek to maximize or minimize *FNP*, or thrust, respectively. Meanwhile, modes 2 and 3 are required to maintain a constant referenced level of thrust as an optimization constraint. Thus, errors in the *FNP* calculation will affect the results for all the optimization modes.

The entire PSC algorithm is duplicated for left and right propulsion systems, and no cross communication exists between the models, identification, or

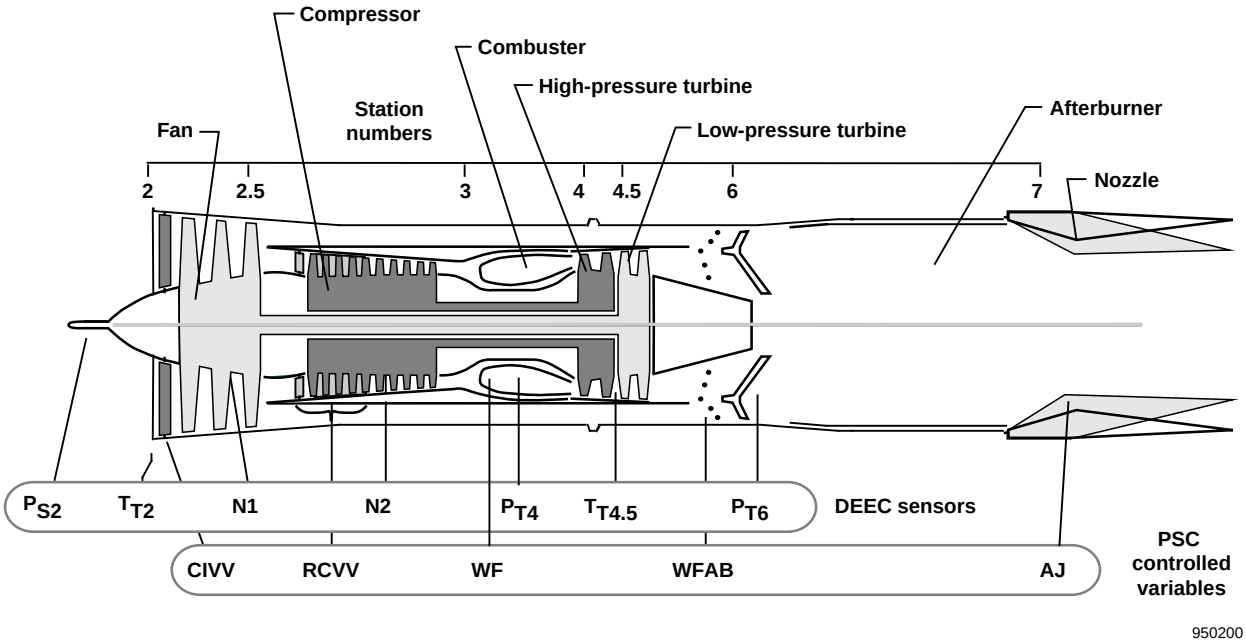

Fig. 2. The F100-PW-1128 engine with digital electronic engine control.

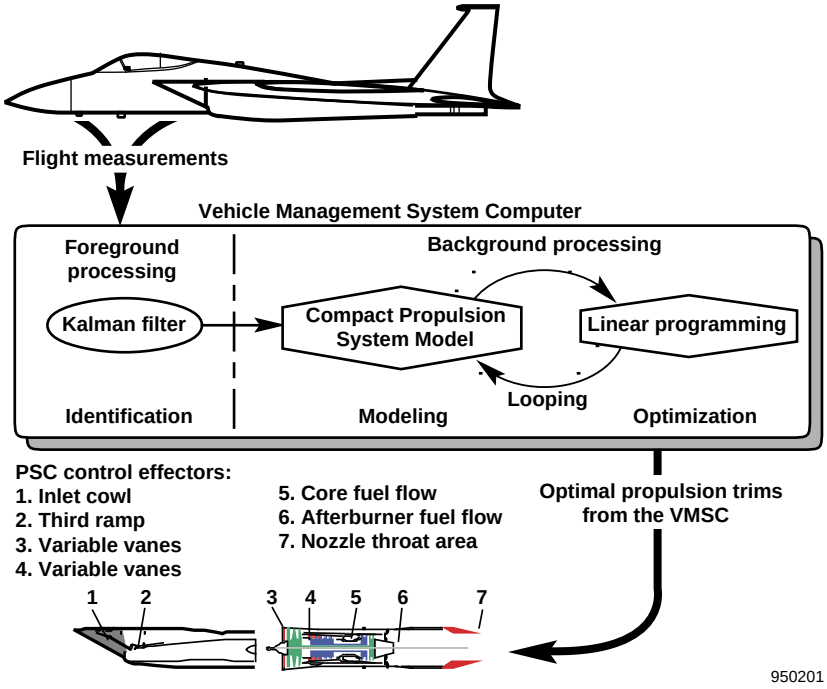

Fig. 3. The PSC implementation and process flow diagram.

optimization. The PSC trims are applied to the propulsion system approximately five times a second subsonically and two times a second supersonically. The reduced trim rate application during supersonic operation is the result of including the large inlet model. Detailed descriptions of the PSC algorithm have been reported,[7, 8, 14] so only selected aspects related to model validation are described in the following subsections.

Identification

The adaptive feature of the PSC algorithm is primarily provided by a Kalman filter (Kf), which attempts to match an onboard compact propulsion system model (CPSM) to the characteristics of the actual engine. The filter estimates five component deviation parameters (CDP) that represent deviations from nominal engine operation. These parameters consist of low spool efficiency adder, high spool efficiency adder, fan airflow adder, compressor airflow adder, and high turbine area adder.[15] Input to the Kf was constrained to the suite of sensors for the standard DEEC measurements (fig. 2).

Kalman filter estimates of the CDP comprise a set of intermediate variables passed to the modeling portion of the PSC algorithm. The model is incrementally adjusted with the CDP to more nearly accurately match measured engine operation. This adaptive feature allows for the PSC optimization to be applied to any F100 series engine independent of state of degradation.

The CDP are defined to be zero for a nominal engine (that is, an engine exactly like the model). The CDP are sensitive to any measured difference from the nominal engine including engine-to-engine variations, engine deterioration, measurement bias, Reynolds effects, and modeling errors.[5] The influence of any single effect on the CDP cannot be identified because of the limited number of measurements available from the standard DEEC.[16]

Modeling

The second major component of the PSC algorithm is the CPSM. The CPSM integrates separate steady-state models of the engine and inlet. The engine model consists of the piece-wise linear Steady-State Variable Model (SSVM) and nonlinear engine model. The current linear point model is scheduled with flight measurements. The CDP are included as input to the SSVM to improve modeling accuracy.

The SSVM is the only part of the modeling to be adjusted with input from the Kf. Engine parameter sensitivity to changes in control effectors and CDP is stored for each point model. Because the PSC controller usually trims the engine off its nominal operating line,

the SSVM also accounts for off-nominal engine operation.*

Following completion of the linear SSVM calculation, additional nonlinear calculations are made. Nonlinear calculations use a combination of analytical equations and empirically derived data tables. Input to the nonlinear routines includes measurements and SSVM output. If a variable is both measured and estimated, the flight measurement is used in the nonlinear calculations. Among the nonlinear output are *FNP*, its force components, and SMF. Net propulsive force and SMF are important parameters for the PSC optimization.

A compact inlet model provides calculated inlet performance for the variable three-ramp F-15 inlet. During subsonic operation, inlet performance is characterized by inlet pressure recovery and inlet spillage drag. Because the inlet ramps are considered optimized for subsonic operation, the inlet ramps are not commanded by PSC subsonically. At supersonic conditions, however, PSC commands the inlet ramps to achieve the desired performance goal. For supersonic operation, inlet performance includes incremental stabilator trim drag and the inlet stability margins of shock displacement ratio and percent critical mass flow. Because of the additional performance considerations at supersonic conditions, the CPSM includes a more complicated and detailed version of the F-15 inlet model during supersonic operation. Integration of the engine and inlet is accomplished by passing the SSVM output of fan airflow to the inlet model as an input, and inlet model-estimated pressure recovery is sent to the SSVM and nonlinear engine model.

Optimization

Information of the CPSM-modeled plant is passed to the optimization logic for optimal trim determination. Certain CPSM output variables are treated as constraints. Others are treated as an objective or cost function. The *FNP* is used as an equality constraint for the minimum fuel and minimum turbine temperature modes. Maximum *FNP* and minimum *FNP* are the objectives of the maximum thrust and rapid deceleration modes, respectively. Certain important constraints, such as SMF, must not be allowed to become negative. A feasible solution (that is, one that does not violate any of the constraints) is sought by the optimization logic with successive calls to the CPSM between trim application.

Optimal trims are applied when the objective function improves and after a predetermined number of calls to the CPSM, referred to as looping. Optimal trim rate depends upon flight condition and the number of loops. At subsonic conditions, there are six loops to each optimization cycle. At supersonic conditions, there are three loops per cycle. It takes longer to complete three loops supersonically than it does to complete six loops subsonically. This difference is primarily caused by inclusion of the larger compact inlet model and the additional controls for inlet ramps and afterburner fuel flow. Timing of the six-loop subsonic operation was between 0.2 to 0.3 sec. For the supersonic three-loop process, timing was between 0.5 and 0.7 sec.

Net Propulsive Force Assessment Technique

Because the *FNP* calculation is given special attention in this report, a closer look at the calculation is warranted. Referring to figures 4(a)–4(e), calculations for gross thrust (F_G), ram drag (F_R), nozzle drag (D_{NOZ}), inlet drag (D_{INL}), and incremental stabilator drag (D_{STAB}) are combined in equation 1 to define *FNP*.

$$FNP = F_G - F_R - D_{NOZ} - D_{INL} - D_{STAB} \qquad (1)$$

The different propulsion-related forces in equation 1 are assumed to act along the flightpath. This assumption is reasonable for low angles of attack.

The PSC method of in-flight thrust calculation, like the TTW, is derived from an energy balance through the engine and uses measured parameters as well as known engine characteristics. As adopted for application to the F100-PW-1128 engines, inputs to the TTW calculation were limited to available production instrumentation. Thus, a number of inputs to the TTW calculation are taken directly from the SSVM outputs. These parameters are the model predicted fan airflow (W_{Cfan}), augmentor inlet total temperature (T_{T6}), combustor exit total pressure (P_{T4}), and engine face total pressure (P_{T2}). Table lookups, analytical gas dynamic equations, and empirically derived equations are used in the computation of F_G.

The F_R is defined and calculated as the product of true airspeed, V_T, and fan airflow, W_{fan}. The D_{NOZ} is modeled as a table look-up of wind-tunnel jet effects data and scheduled with flight-measured input. The D_{INL} is composed of three drag terms: C_{Dtrim}, C_{Dpb}, and C_{Decs}. The inlet spillage drag combined with trim drag is modeled and referred to as C_{Dtrim}. The plenum bleed

*Yonke, William A. and Nobbs, Steven G., *Performance Seeking Control (PSC) Final Report*, MDC 94B0003, McDonnell Douglas Aerospace, St. Louis, Missouri, Jan. 1994. This report is not available to the public. Contact the authors with queries regarding this report.

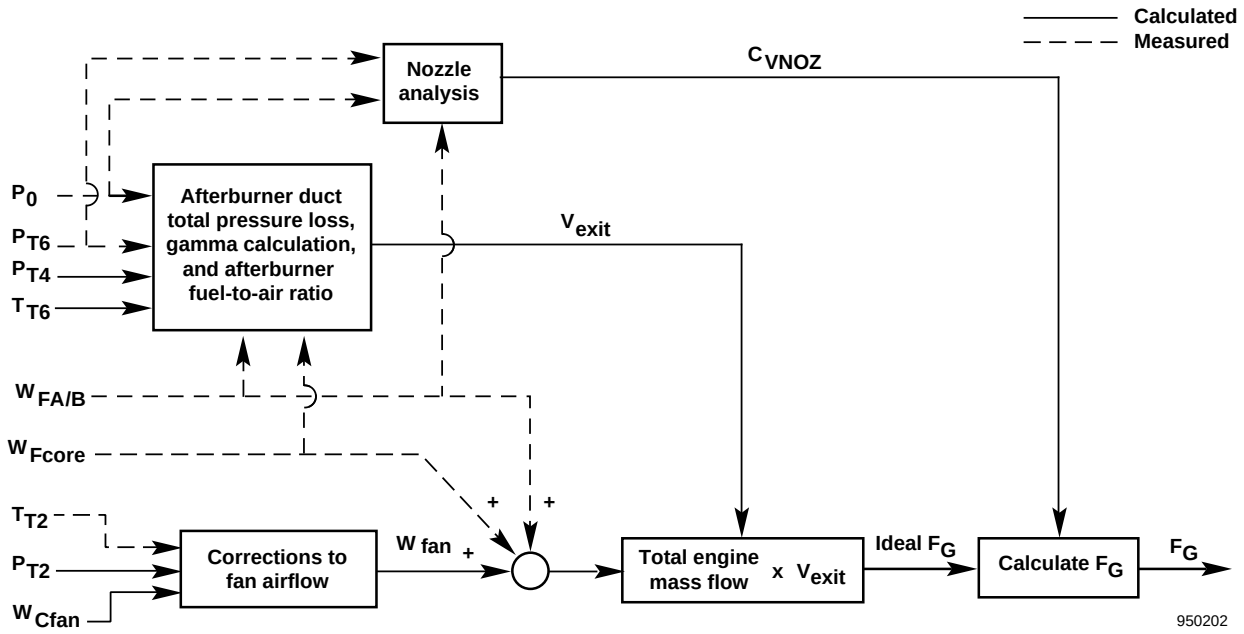

(a) Gross thrust.

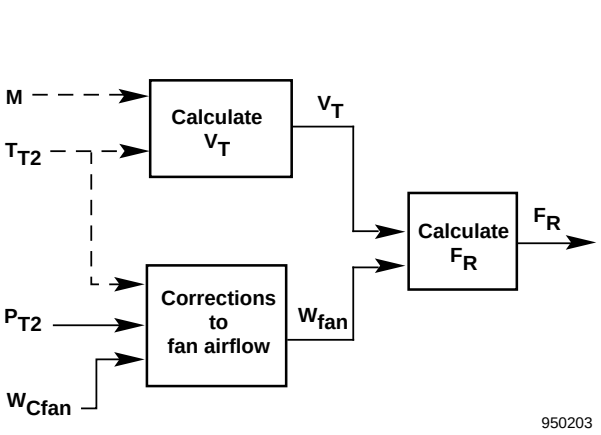

(b) Ram drag.

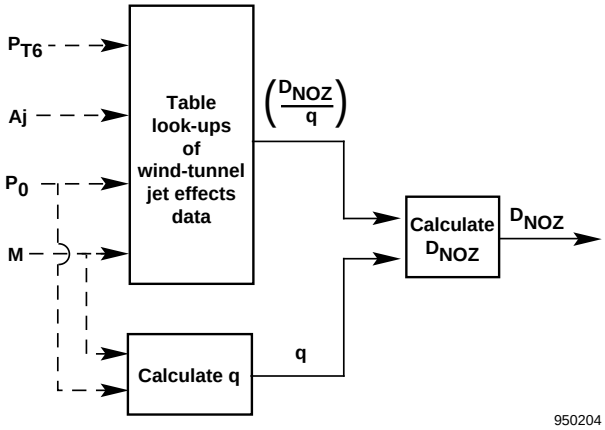

(c) Nozzle drag.

Fig. 4. The PSC onboard in-flight thrust model.

drag (C_{Dpb}) calculation involves complicated geometric relations between the variable inlet ramps and flight conditions. Calculation of the final inlet drag term involves table lookups to account for environmental control system drag (C_{Decs}), drag which is associated with the bleeding of air from the inlet. The incremental stabilator drag component of *FNP* accounts for the coupling of the propulsion system with the airframe. If the inlet is trimmed to an off-scheduled position, an incremental lift is produced, thus imparting a pitching moment on the airframe. To offset the pitching moment and maintain level flight, the stabilator is used. Stabilator is repositioned to produce a counteracting pitching moment; however, stabilator drag is also affected. The D_{STAB} is defined as the incremental stabilator trim drag plus the incremental inlet drag. Both of these drags are associated with moving the cowl off-schedule. Note that the stabilator is not directly controlled by PSC but rather depends on the autopilot or pilot to trim out the pitching moments. Wind-tunnel

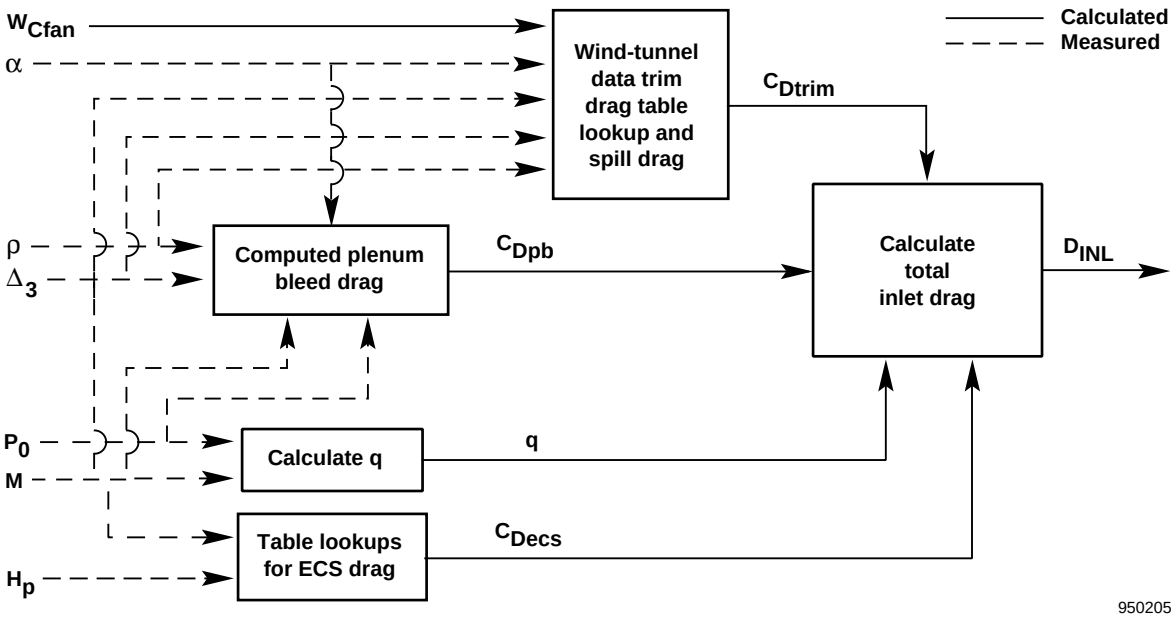

(d) Inlet drag.

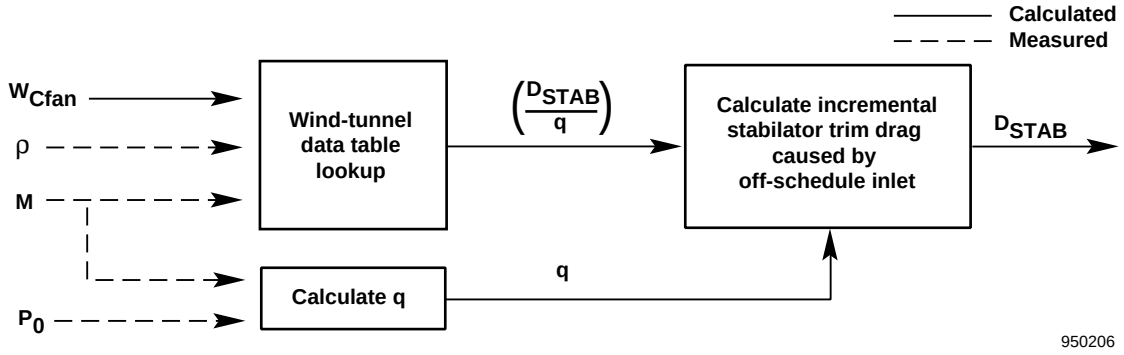

(e) Incremental stabilator drag.

Fig. 4. Concluded.

data of D_{STAB} are computed with table lookups and scheduled with measurements and SSVM variables.

Excess Thrust Method

The accuracy for the onboard PSC *FNP* estimate was assessed with an analysis of aircraft excess thrust, F_{ex}. The analysis technique consists of a comparison between modeled and measured increases in longitudinal force from maximum thrust mode acceleration tests. For 1-*g* flight, *FNP* relates to longitudinal acceleration, N_x, through the following expression:

$$F_{ex} = FNP - D = N_x \times Wt \qquad (2)$$

where *D* represents total aircraft drag excluding the propulsive drag terms.

The method chosen to evaluate modeled *FNP* accuracy compares back-to-back, 1-*g* accelerations with and without PSC engaged in the maximum thrust mode. A significant increase in acceleration was experienced. The first acceleration was completed as a baseline, and the second was completed with the PSC maximum thrust mode engaged. With PSC engaged, predicted increases in *FNP* from the baseline were also reflected as measured increases in N_x. From equation (2) during such PSC operation, only the aircraft drag term, *D*, is unknown. However, because none of the PSC trims directly influence airframe drag, changes in drag

between the two accelerations are assumed to be zero; that is, $\Delta D = 0$. Then, the following expression relates an increase in *FNP* with an associated increase in N_x:

$$\Delta F_{ex} = \Delta FNP = \Delta(N_x \times Wt) \quad (3)$$

During in-flight tests, a conventional linear accelerometer measures N_x, but there is no instrument available to measure *FNP*. For this reason, two calculations of ΔF_{ex} will be made, one based on measured N_x, $\Delta F_{ex_{meas}}$, and one from modeled *FNP*, $\Delta F_{ex_{model}}$ according to equations 4 and 5.

$$\Delta F_{ex_{model}} = \Delta FNP = FNP_{on} - FNP_{off} \quad (4)$$

and

$$\Delta F_{ex_{meas}} = \Delta(N_x \times Wt) = (N_x \times Wt)_{on} - (N_x \times Wt)_{off} \quad (5)$$

where *on* and *off* refer to acceleration data with and without the PSC maximum thrust mode engaged. Aircraft gross weight, *Wt*, is calculated as the sum of zero fuel weight, Wt_0 and total indicated fuel, Wt_f.

Differences between the measured and the modeled ΔF_{ex} represent modeling error. Ideally, modeling error may be presented as a percentage of measured values; however, any percentage error calculation containing a denominator that approaches zero may be misleading. As described in the Results and Discussion section, the $\Delta F_{ex_{meas}}$ levels approach zero at some flight conditions. Thus, calculations with $\Delta F_{ex_{meas}}$ in the denominator will be inflated. To alleviate the potential for misinterpreting the results, modeling accuracy will be presented in terms of percentage of full-scale measured F_{ex}. The $F_{ex_{meas}}$ value is taken from the test completed without the PSC optimization selected, or $(N_x \times Wt)_{off}$. Keep in mind the percentage difference (*PD*) value does not represent conventional modeling error. Note also that *PD* values are less than percentage error values. The *PD* was calculated according to equation 6.

$$PD = [(\Delta F_{ex_{model}} - \Delta F_{ex_{meas}})/(N_x \times Wt)_{off}] \times 100 \quad (6)$$

A secondary benefit of reporting modeling accuracy in terms of full-scale F_{ex} is that *PD* analysis results can be directly applied to the prior PSC findings. For example, prior findings identified a 10 percent ΔF_{ex} increase for maximum thrust mode operation at Mach 0.7 and an altitude of 30,000 ft. The *PD* results indicate a 2 percent level of ΔF_{ex} modeling accuracy at this condition. Thus, bounds on the optimization results may now be given. The maximum thrust mode achieves between an 8- to 12-percent increase in F_{ex}.

Test Conditions

Accelerations were conducted for the PSC maximum thrust mode at two power settings and three altitudes. Flight test data are acquired from onboard instrumentation of PSC model outputs and sensor readings. Table 1 summarizes the conditions for the tests.

Table 1. Test conditions.

Test point	Power setting	Altitude, ft	Mach number range
1	Mil	30,000	0.50 to 0.95
2	Max	30,000	0.60 to 1.60
3	Max	45,000	0.80 to 2.00

Data Standardization

Data standardization and corrections to reference conditions are addressed before performance data are to be analyzed. The *FNP* validation test points were flown in sets of two through the same air mass at an equivalent altitude. This procedure was used to reduce the influences of changing atmospheric conditions on propulsion system operation and aircraft drag; however, aircraft total drag differed noticeably between the two accelerations because of differences in aircraft weight. These drag differences require standardization of measured test day excess thrust to a standard weight condition. A simplified performance model of the F-15 aircraft was used to accommodate changes in aircraft drag resulting from differences in aircraft mass.[17] Error bands associated with this method previously developed for quantifying acceleration performance improvements[10] should be less than 1.4 percent at an altitude of 45,000 ft and 3.4 percent at an altitude of 30,000 ft. The PSC_{off} weight was selected as the standard weight to which the PSC_{on} test data were corrected. The following correction was applied to test day $(N_x \times Wt)_{TEST}$ with PSC_{on} to obtain $(N_x \times Wt)_{on}$:

$$(N_x \times Wt)_{on} = (N_x \times Wt)_{TEST} + \Delta D_{CORR} \quad (7)$$

where $\Delta D_{CORR} = D'_{off} - D'_{on}$. The D' is the postflight model predicted drag. Errors in the drag correction are expected to be small. Only the difference in modeled drag is being applied as a correction.

Uncertainty Analysis

Measurement uncertainty of $\Delta F_{ex_{meas}}$ must be known if $F_{ex_{meas}}$ is to be considered the true value of comparison for $\Delta F_{ex_{model}}$. To that end, an uncertainty analysis was performed to gauge the significance of measurement errors on the $\Delta F_{ex_{meas}}$ calculation. Table 2 lists the measured inputs to the $\Delta F_{ex_{meas}}$ calculation. Measurement of N_x has a manufacturer's quoted precision of ±0.50 percent full-scale. The precision of the total indicated fuel weight, Wt_f was ±3.50 percent full-scale. Aircraft empty weight, obtained in special weight and balance tests, has a ±0.07 percent full-scale precision.

Measurement uncertainty of $\Delta F_{ex_{meas}}$ was less than 1.15 percent at test condition 1. This test represents typical data to be analyzed for excess thrust modeling accuracy. Levels of uncertainty are expected to be similarly small for the other test conditions.

Table 2. Measurement ranges and uncertainties of ΔF_{ex} input parameters.

Parameter	Range	Uncertainty, percent of full scale
N_x	–1 to 1 *g*	±0.50
Wt_0	0 to 280,000 lb	±0.07
Wt_f	0 to 10,800 lb	±3.50

Fan Stall Margin Assessment Technique

Engine stability margin is expressed in terms of stall margin remaining. Stall margin is defined as the difference between the stall and operating pressure ratio, at constant airflow, divided by the reference (operating) pressure ratio. Stall margin may be defined for the fan and for the compressor, but only the SMF is described in this report. Fan stall margin is one of the critical parameters output from the CPSM. This margin is used as a constraint during the optimization process. Calculated stall margin must never be allowed to become negative while optimizing the selected performance index. A negative calculated stall margin may cause the engine to stall. The intentional fan stall test was conducted to quantify the overall accuracy of the PSC SMF model.

Much of the performance gain achieved by PSC at subsonic speeds is accomplished by uptrimming the engine pressure ratio (*EPR*), effectively increasing the fan pressure ratio (*FPR*). If *FPR* is increased at a constant airflow, then stall margin is reduced (fig. 5(a)). Reduced stall margin was observed and reported for three of the PSC optimization modes,[7] especially at subsonic flight conditions. Individual components of the stall margin calculation can not be assessed because of the insufficient information available during flight test. Even so, reviewing the methodology of the PSC SMF model to understand the possible sources of error is worthwhile.

The PSC incorporates the PW stability audit methodology that assesses the effects shown in figure 5(a) to predict SMF. Base stall line data obtained from engine testing at Arnold Engineering Development Center (AEDC) (Tullahoma, Tennessee) of a one-sixth scale F-15 model in 1970–1971 were tabulated and stored onboard the VMSC.[1] A base stall line definition is determined in real-time with SSVM-corrected fan airflow as input to a table lookup. The base stall line is adjusted by a Reynolds factor (ΔFPR_{Re}), *CIVV* factor (FPR_{CIVV}), random effects, η, and distortion effects (ΔFPR_{dis}) to calculate the installed stall line. The ΔFPR_{Re} accounts for off-design airflow temperature and density. A decrease in Reynolds number lowers the fan stall line by decreasing its fan pressure ratio, *FPR*. The FPR_{CIVV} describes the effects of off-schedule guide vanes. Opening the variable guide vanes of the fan reduces the *FPR* of the stall line. The random effects include a 1-percent margin for engine-to-engine variations and a 1-percent margin for control tolerances.

Because there are no known means of determining random effects in-flight, η is fixed at a constant 2 percent. Distortion effects are made to adjust the stall line for distorted airflow entering the engine face. The PSC uses an inlet distortion model which takes into account angle of attack, α, angle of sideslip, β, Mach number, and compressor inlet variable vane angle. Tabulated results from the AEDC tests were incorporated as part of the PSC inlet distortion model. An increase in ΔFPR_{dis} also causes the stall line *FPR* to be reduced. All decrements to the base stall line are determined in real-time by the PSC model.

Besides adjustments to the base stall line, a fixed amount of stall margin buffer is added to the nominal operating line. Pratt & Whitney suggested this addition as a safety precaution to prevent stalling because of uncertainties in the audit methodology and to increase the buffer against the statistical nature of stalls. Implementation of the minimum allowable stall margin remaining has been as a fixed value of 4 percent at all dry power settings and 6 percent at maximum afterburner power. At partial afterburner power settings,

the limit is increased to 10 percent because of stability concerns about augmentor sequencing. For example at maximum afterburner power, at an airspeed of Mach 0.9, and an altitude of 30,000 ft, an approximately 18-percent stall margin is available for uptrimming (fig. 5(b)).

The final installed stall line is defined as

$$FPR_i = FPR_{CIVV} \times [1 + \Delta FPR_{Re}] \times [\eta] - \Delta FPR_{\text{dis}} \quad (8)$$

Figure 6 shows the inputs and calculation process for FPR_i. The operating fan pressure ratio is defined as

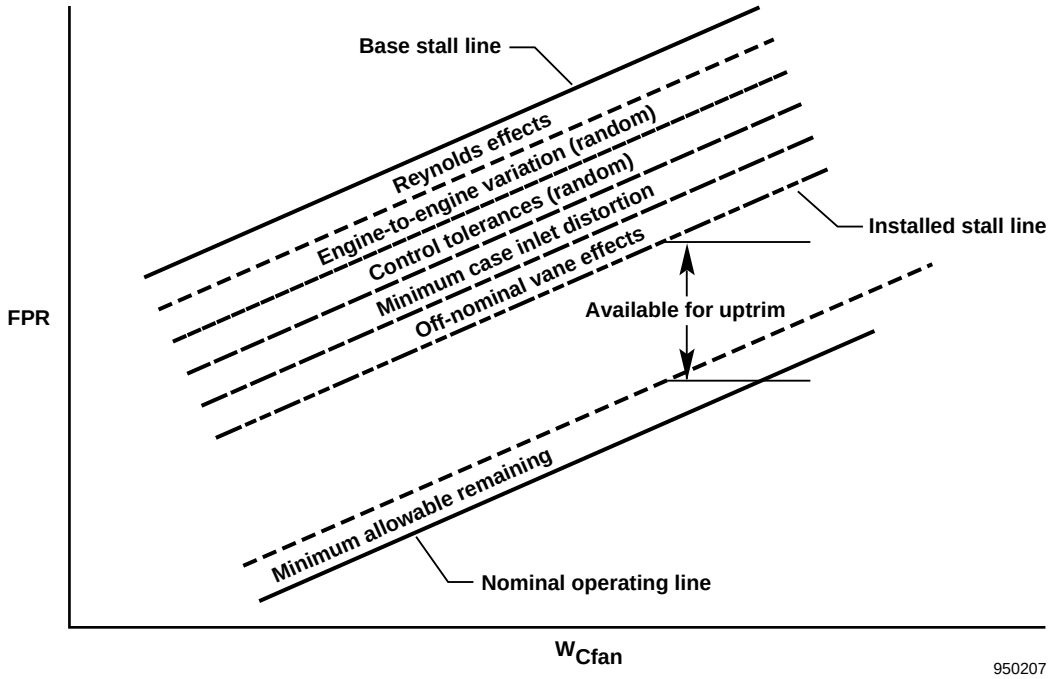

(a) Typical operating conditions.

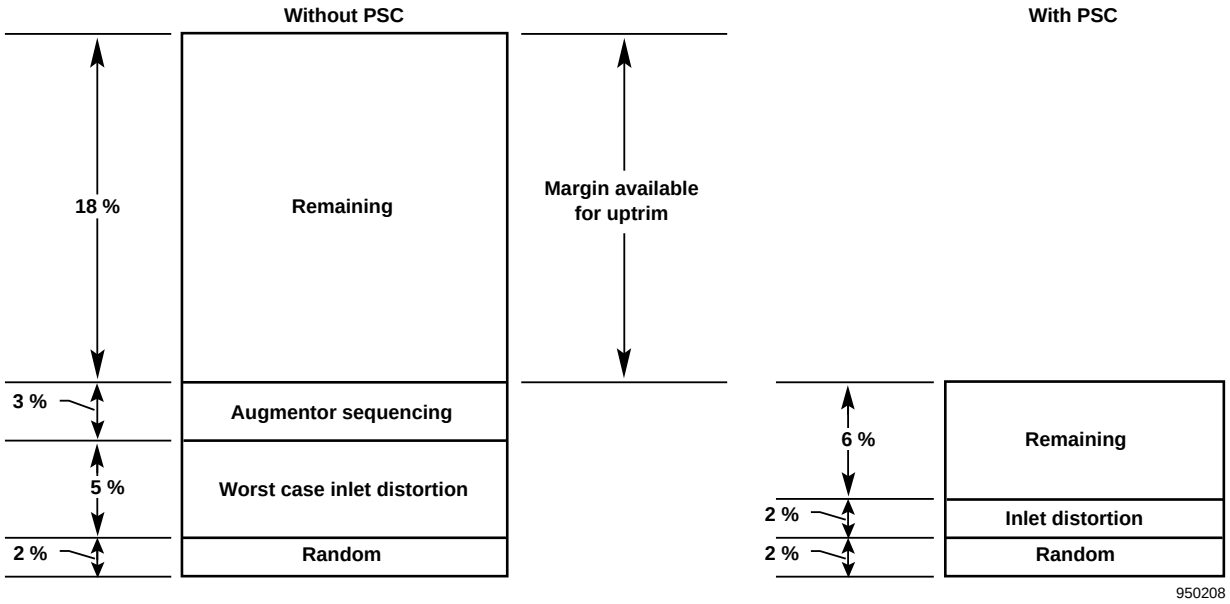

(b) Stall margin available for maximum afterburner power at Mach 0.9 and an altitude of 30,000 ft during cruise.

Fig. 5. Fan stall margin audit for the F100-PW-1128 engines during the PSC program.

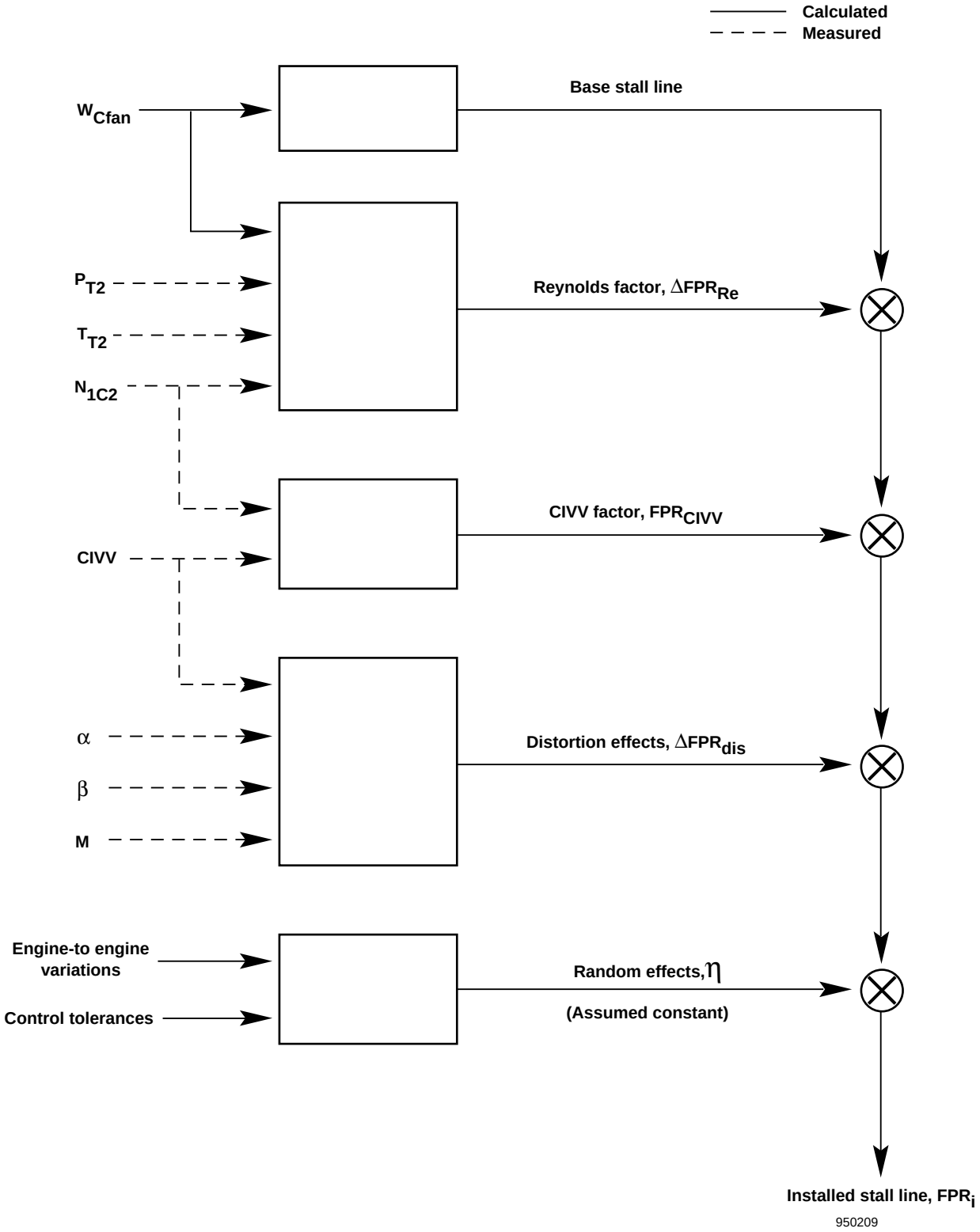

Fig. 6. The PSC onboard in-flight installed stall line calculation.

$$FPR_o = P_{T2.5}/P_{T2} \quad (9)$$

where $P_{T2.5}$ is determined from the SSVM, and P_{T2} is output from the compact inlet model. Fan stall margin is defined as

$$\text{SMF} = [FPR_i - FPR_o]\,/FPR_o \quad (10)$$

Intentional Fan Stall Method

Procedurally, fan stalls must be intentionally induced because the PW F100 class of engines are proven to be robust with respect to encountering stall and are very unlikely to stall without some assistance. Errors in estimated SMF will be determined by comparing SMF values at the time of a stall event. To reduce the likelihood of a single bad data point, the test was repeated so that a total of four stalls were evaluated.

Test Conditions

A steady-state cruise flight condition of Mach 0.9 and altitude of 30,000 ft was chosen as the test condition to minimize the effect of outside factors and allow for a very controlled test. For the test engine to be stalled, power was set at maximum afterburner, while the other, nontest engine was modulated to maintain constant Mach number. A preprogrammed set of progressively increasing *EPR* trim values was selected until a fan stall was detected. Mach 0.9 and an altitude of 30,000 ft is the engine design point. At this condition, no ΔFPR_{Re} adjustment is made. Inlet distortion is expected to very small at this condition. The variable vanes are on schedule and not trimmed so that no FPR_{CIVV} adjustments will be made. With these conditions, the SMF model provides its most accurate estimates.

Results and Discussion

Test results of the excess thrust test and the intentional fan stall test are discussed in the following subsections. The tests were designed to assess the *FNP* and SMF modeling accuracy of the PSC algorithm.

Excess Thrust Test

Figure 7 shows a comparison of two back-to-back accelerations for test condition 1 with and without the PSC maximum thrust mode selected. The curve labeled PSC_{on} is with maximum thrust mode selected. The curve labeled PSC_{off} is without maximum thrust mode selected. Time to accelerate from Mach 0.5 to Mach 0.95 is reduced by 12 sec or about 15 percent with PSC, as illustrated by the PSC_{on} curve of figure 7(a). The roughly 0.03-*g* increase of N_x (fig. 7(b)) results from significant increases in *FNP* (fig. 8(a)). The *FNP* gains are achieved by uptrimming the engine and operating with reduced SMF (fig. 7(c)).

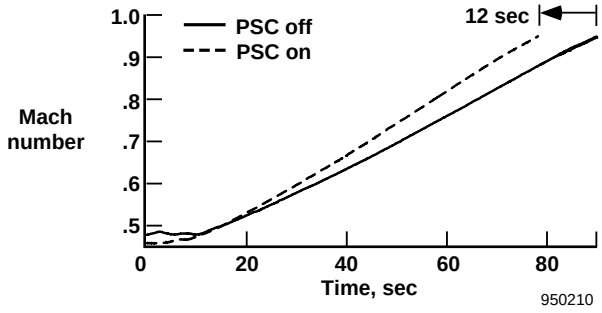

(a) Measured Mach number.

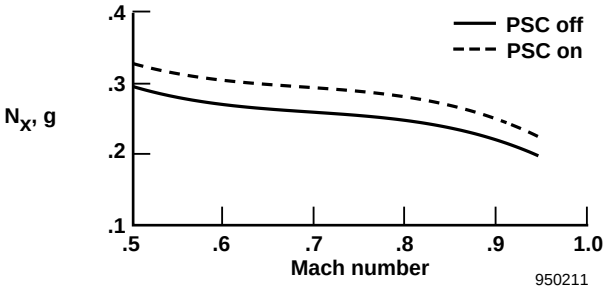

(b) Measured longitudinal acceleration.

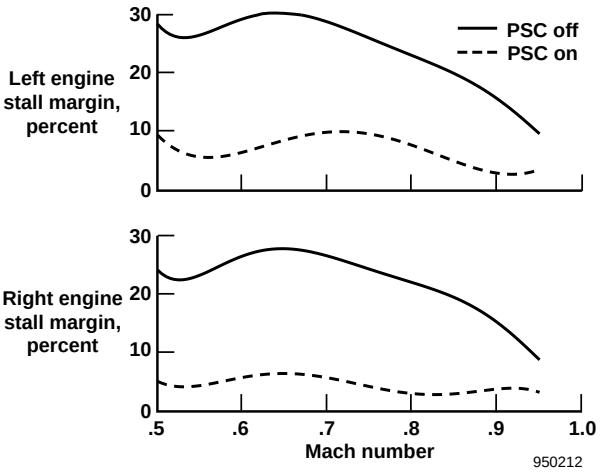

(c) Modeled fan stall margin.

Fig. 7. Maximum thrust mode optimization results at test condition 1.

The model and the measured values of F_{ex} show sustained increases from PSC maximum thrust mode application for most of the run. Measured increase in

F_{ex} is nearly 1000 lb at Mach 0.7 (fig. 8(b)). At the same Mach number, the model predicts 850 lb of increase in *FNP* (fig. 8(a)). Throughout the acceleration, $\Delta F_{ex_{model}}$ is predicted less than $\Delta F_{ex_{meas}}$. A maximum temperature limit causes the F_{ex} increases to taper off somewhat near the end of the acceleration.

Figure 8(c) illustrates the *PD* between measured and modeled ΔF_{ex}. Model accuracy is at 2 percent or less of measured baseline excess thrust for most of the Mach number range. As Mach 0.95 is approached, *PD* increases to nearly 4 percent. Modeling accuracy is expected to degrade above Mach 0.95 where the value and uncertainty in propulsion system drag increase.

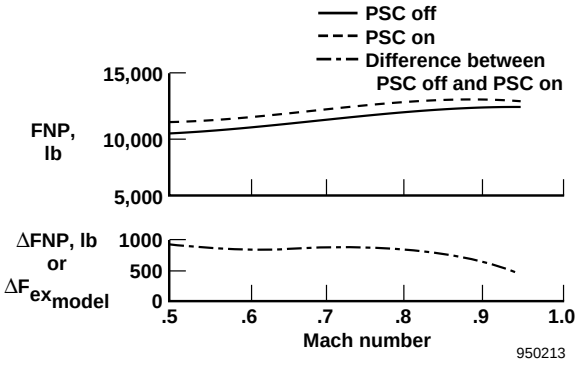

(a) Modeled increase in *FNP*.

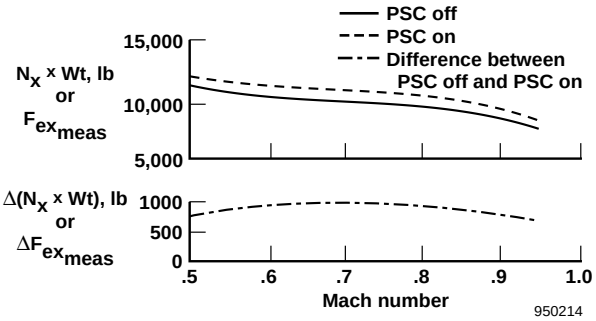

(b) Measured increase in F_{ex}.

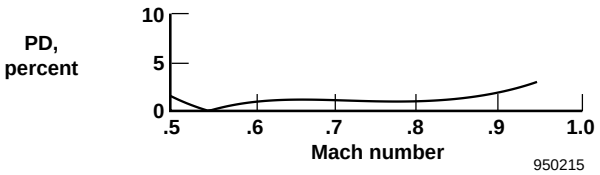

(c) Percent difference of modeled to measured increase in excess thrust.

Fig. 8. Excess thrust results at test condition 1.

Figures 9(a)–9(c) present comparison plots of the measured to modeled ΔF_{ex} and *PD* for test condition 2. The ΔF_{ex} levels lie between zero near Mach 1.0 and 2000 lb at higher Mach numbers. The level of accuracy is less than 2 percent from low subsonic until around Mach 1.3. At which point, modeling accuracy worsens to reach about 10 percent above Mach 1.45.

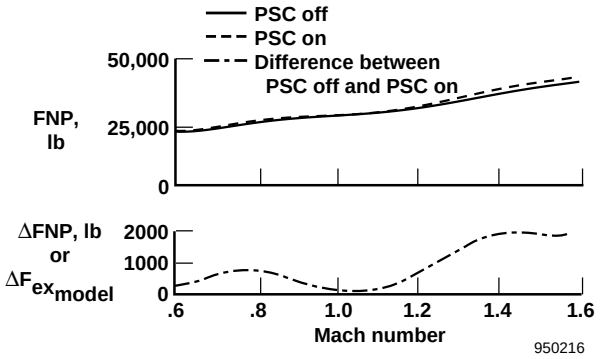

(a) Modeled increase in *FNP*.

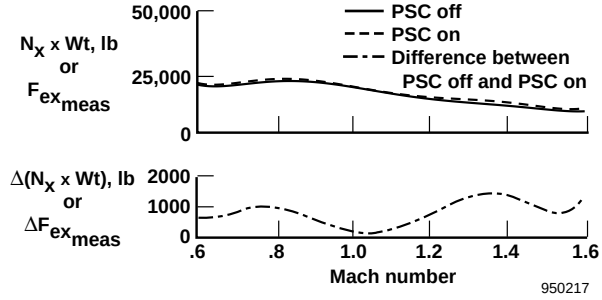

(b) Measured increase in F_{ex}.

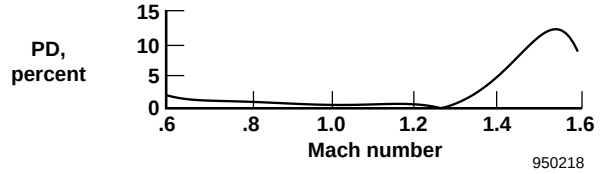

(c) Percent difference of modeled to measured increase in excess thrust.

Fig. 9. Excess thrust results at test condition 2.

Results for test point 3 show F_{ex} increases of about 1000 lb for most of the acceleration (figs. 10(a)–10(c)). Modeling accuracy is generally within 3 percent below Mach 1.7. From Mach 1.7 to Mach 2.0 the level of

accuracy steadily deteriorates with a maximum difference of over 10 percent at Mach 2.0.

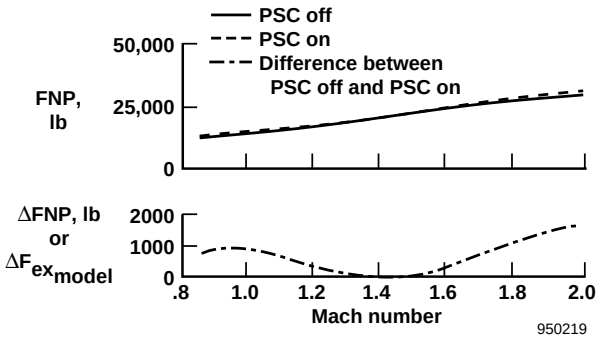

(a) Modeled increase in *FNP*.

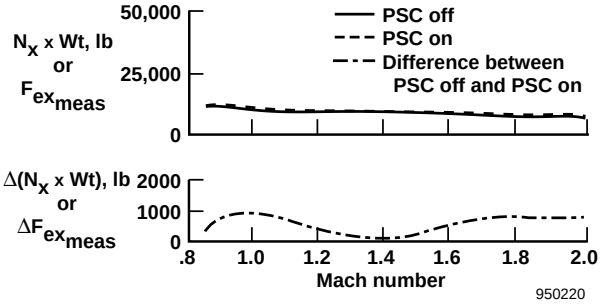

(b) Measured increase in F_{ex}.

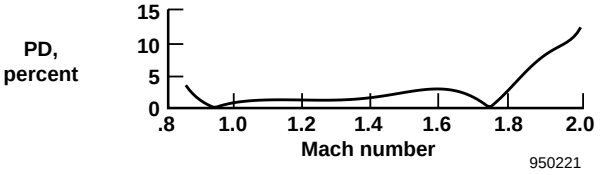

(c) Percent difference of modeled to measured increase in excess thrust.

Fig. 10. Excess thrust results at test condition 3.

Numerous possible sources of error in the Δ*FNP* calculation exist. The *FNP* calculation represents the most complicated parameter output from the PSC model and relies upon more measurements and model inputs than any other PSC calculated parameter. Contributions to absolute *FNP* error caused by specific measurement inaccuracies and unmodeled physical phenomena are extremely difficult to quantify, especially from data gathered in-flight. This analysis makes no attempt to identify and specify distinct sources of error. Such an analysis is beyond the scope of current activity; however, absolute *FNP* error will be partially offset when taking differences between absolute levels of *FNP* and making comparisons of Δ*FNP* or ΔF_{ex}.

All three of the tests analyzed demonstrate modeling accuracy to be within 3 percent or less for the majority of each acceleration. Each test case displayed similar modeling error behavior. Toward the end of each acceleration, modeling accuracy deteriorated beyond the 3-percent levels to as much as 10 percent. The errors discovered with the excess thrust technique represent combined model errors of the numerical representations of the unique left and right propulsion systems. As a result, excess thrust model error is not be expected to be exactly the same for other propulsion systems with the same class of engines. On the other hand, overall trends are expected to be similar.

Intentional Fan Stall Test

Using the intentional fan stall methodology, four engine stalls were induced, three on the left engine and one on the right. Figure 11 depicts time traces of estimated stall margin from before the *EPR* uptrim is applied until the moment of stall at which time model execution is halted. The model predicts a zero stall margin when the fan operating point crosses the adjusted stall line. At the test conditions, adjustments to the base stall line are made only for inlet distortion and random effects.

Left engine stalls occurred when *EPR* was uptrimmed by 26 and 30 percent. As shown in figures 11(a)–11(c), calculated SMF varied between –9.5 and –10.2 percent for the left engine at the point stall occurred. Comparing the stall events, differences of the *EPR* uptrim required to induce stall and of estimated stall margin at the point of stall may be explained by the statistical nature of stall phenomena. Taken together, results from each stall event show the SMF model for the left engine contains errors of approximately 10 percent at this test condition.

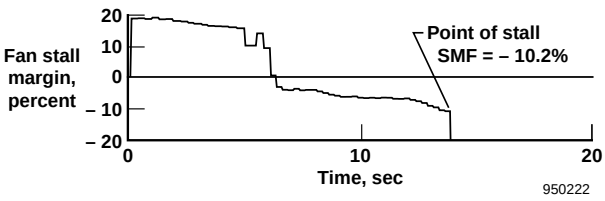

(a) Left engine with a 26 percent *EPR* uptrim.

Fig. 11. Fan stall margin test results.

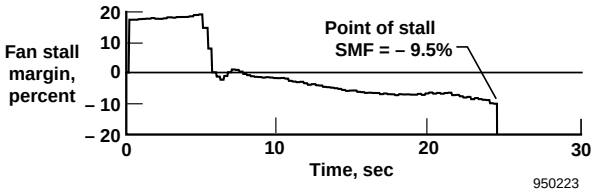

(b) Left engine with a 26 percent *EPR* uptrim.

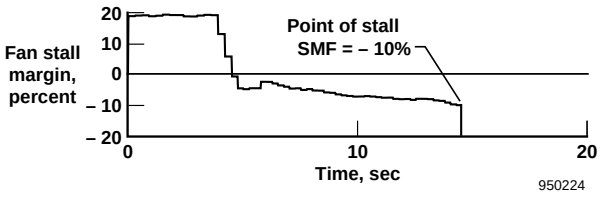

(c) Left engine with a 30 percent *EPR* uptrim.

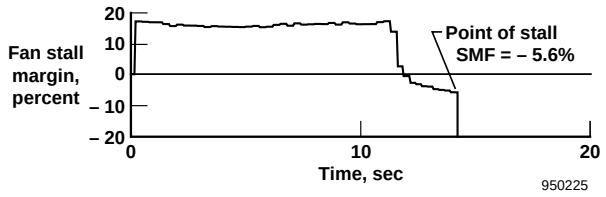

(d) Right engine with a 30 percent *EPR* uptrim.

Fig. 11. Concluded.

Figure 11(d) shows the right engine stall event. The stall occurred much sooner after *EPR* uptrim application than was the case with the left engine. Detected SMF error at the time of stall was –5.6 percent or about one-half of the error seen with the left engine model. Modeling differences were expected because of the operating differences between these engines.

The possible sources of SMF model error include calculated fan airflow, inlet and exit total pressures as well as measurement errors. The assumption of constant random effects introduces some level of error, however, not at levels high enough to resolve the detected error. Modeled $P_{T2.5}$ has been previously reported on to be within 2 percent of measured at this flight condition, so $P_{T2.5}$ model error will contribute some of the model error in SMF. Fan airflow, W_{Cfan}, is very sensitive to unmodeled sensor bias and the Kf CDP estimates. The model estimate for fan airflow has been reported to be as high as 5 lb/sec higher than the DEEC-calculated airflow. Pratt & Whitney believe the PSC model provides a more accurate value.[4, 5] Errors in model airflow will appear as errors in stall margin through the base stall line table lookups.

Differences between the left and right stall margin model errors may be explained between physical differences between the engines. For example, the left engine generally operated at higher turbine temperature for a given fan speed, thus indicating a more deteriorated engine. Nonwhite noise and bias characteristics differ between individual sensors located on the left and right engines and will contribute to the effects of unmodeled sensor errors.

Results showing that SMF error is always negative imply that at given level of calculated stall margin, there is in reality an extra amount of stall margin available before the fan will stall. This built-in conservatism may have prohibited PSC from achieving optimal performance improvements. Three of the PSC optimization modes drive the SMF to its constrained minimum stall margin remaining value.[7] Pratt & Whitney suggested that a 5-percent reduction in SMF design requirements could lead to thrust-to-weight increases of 3 percent or translate to a 1.2-percent fuel burn reduction. Clearly, one way to achieve increased performance at levels exceeding the performance improvements demonstrated with PSC is by improving modeling accuracy.

Conclusions

The Performance Seeking Control (PSC) algorithm, a model-based, adaptive control algorithm, was flight tested with built-in models of the engine and the inlet. Flight results show substantial performance improvements from the F-15 PSC algorithm. Because these benefits are determined from the PSC modeling, demonstrated results are only as accurate as the models. As a result, assessing and quantifying the modeling accuracy of the PSC algorithm is critical.

A method of determining PSC model accuracy for the estimation of increases in net propulsive force, *FNP*, was developed and applied to flight test data. This method, the excess thrust technique, has been applied to assess the *FNP* model. Results show that measured increases of *FNP* are generally accurate to within 3 percent of full-scale excess thrust. Accuracy to these levels is significant to the estimated performance improvements provided by PSC in all of its optimization modes. The *FNP* is used in each of the optimization modes. With an assessment of changes in *FNP* accuracy, uncertainty bands may now be applied to the optimization results.

The second test to evaluate PSC modeling accuracy involved intentionally stalling the fan. Results indicate that the PSC model is excessively conservative, and the modeling accuracy is within the –5- to –10-percent range for fan stall margin. With improved stall margin modeling capability, PSC may have achieved larger performance improvements than were demonstrated.

References

[1]*Highly Integrated Digital Electronic Control Symposium*, NASA CP-3024, 1987.

[2]Goecke Powers, Sheryll, comp., *An Electronic Workshop on the Performance Seeking Control and Propulsion Controlled Aircraft Results of the F-15 Highly Integrated Digital Electronic Control Research Program, Proceedings of the Electronic Workshop*, NASA TM-104278, 1995.

[3]Beaulieu, Warren, Campbell, Ralph, and Burcham, William, "Measurement of XB-70 Propulsion Performance Incorporating the Gas Generator Method," *J. Aircraft*, vol. 6, no. 4, July–Aug. 1969, pp. 312–317.

[4]Maine, T., Gilyard, G., and Lambert, H., *A Preliminary Evaluation of an F100 Engine Parameter Estimation Process Using Flight Data*, AIAA 90-1921, July 1990.

[5]Orme, J.S. and Gilyard, G.B., *Subsonic Flight Test Evaluation of a Propulsion System Parameter Estimation Process for the F100 Engine*, NASA TM-4426, 1992.

[6]Conners, Timothy, R., *Thrust Stand Evaluation of Engine Performance Improvement Algorithms in an F-15 Airplane*, NASA TM-104252, 1992.

[7]Gilyard, G.B. and Orme, J.S., *Subsonic Flight Test Evaluation of a Performance Seeking Control Algorithm on an F-15 Airplane*, NASA TM-4400, 1992.

[8]Lambert, H.H., Gilyard, G.B., Chisholm, J.D., and Kerr, L.J., *Preliminary Flight Evaluation of an Engine Performance Optimization Algorithm*, NASA TM-4328, 1991.

[9]Orme, J.S. and Gilyard, G.B., *Preliminary Supersonic Flight Test Evaluation of Performance Seeking Control*, NASA TM-4494, 1993.

[10]Orme, John S. and Conners, Timothy, R., *Supersonic Flight Test Results of a Performance Seeking Control Algorithm on a NASA F-15 Aircraft*, AIAA 94-3210, June 1994.

[11]Beeler, De E., Bellman, Donald R., and Saltzman, Edwin J., *Flight Techniques for Determining Airplane Drag at High Mach Numbers*, NACA TN-3821, 1956.

[12]Ray, Ronald J., *Evaluating the Dynamic Response of In-Flight Thrust Calculation Techniques During Throttle Transients*, NASA TM-4591, 1994.

[13]Burcham, Frank W., Jr., Myers, Lawrence P., and Walsh, Kevin R., *Flight Evaluation Results for a Digital Electronic Engine Control in an F-15 Airplane*, NASA TM-84918, 1983.

[14]Smith, R.H., Chisholm, J.D., and Stewart, J.F., "Optimizing Aircraft Performance with Adaptive, Integrated Flight/Propulsion Control," *J. Engineering for Gas Turbines and Power*, vol. 113, Jan. 1991, pp. 87–94.

[15]Luppold, R.H., Roman, J.R., Gallops, G.W., and Kerr, L.J., *Estimating In-Flight Engine Performance Variations Using Kalman Filter Concepts*, AIAA-89-2584, July 1989.

[16]España, Martîn D. and Gilyard, G.B., *On the Estimation Algorithm Used in Adaptive Performance Optimization of Turbofan Engines*, NASA TM-4551, 1993.

[17]Orme, John S., *Digital Performance Simulation Models of the F-15, F-16XL, F-18, F-104, TACT F-111, X-29, and Hypersonic Research Vehicle*, NASA TM-104244, 1992.

REPORT DOCUMENTATION PAGE

Form Approved
OMB No. 0704-0188

1. AGENCY USE ONLY (Leave blank)	2. REPORT DATE	3. REPORT TYPE AND DATES COVERED
	July 1995	Technical Memorandum

4. TITLE AND SUBTITLE

Flight Assessment of the Onboard Propulsion System Model for the Performance Seeking Control Algorithm on an F-15 Aircraft

5. FUNDING NUMBERS

WU 533-02-03

6. AUTHOR(S)

John S. Orme and Gerard S. Schkolnik

7. PERFORMING ORGANIZATION NAME(S) AND ADDRESS(ES)

NASA Dryden Flight Research Center
P.O. Box 273
Edwards, California 93523-0273

8. PERFORMING ORGANIZATION REPORT NUMBER

H-2060

9. SPONSORING/MONOTORING AGENCY NAME(S) AND ADDRESS(ES)

National Aeronautics and Space Administration
Washington, DC 20546-0001

10. SPONSORING/MONITORING AGENCY REPORT NUMBER

NASA TM-4705

11. SUPPLEMENTARY NOTES

Presented as AIAA 95-2361 at the 31st AIAA/ASME/SAE/ASEE Joint Propulsion Conference, San Diego, California, July 10–12, 1995.

12a. DISTRIBUTION/AVAILABILITY STATEMENT

Unclassified—Unlimited
Subject Category 07

12b. DISTRIBUTION CODE

13. ABSTRACT (Maximum 200 words)

Performance Seeking Control (PSC), an onboard, adaptive, real-time optimization algorithm, relies upon an onboard propulsion system model. Flight results illustrated propulsion system performance improvements as calculated by the model. These improvements were subject to uncertainty arising from modeling error. Thus to quantify uncertainty in the PSC performance improvements, modeling accuracy must be assessed. A flight test approach to verify PSC-predicted increases in thrust (*FNP*) and absolute levels of fan stall margin is developed and applied to flight test data. Application of the excess thrust technique shows that increases of *FNP* agree to within 3 percent of full-scale measurements for most conditions. Accuracy to these levels is significant because uncertainty bands may now be applied to the performance improvements provided by PSC. Assessment of PSC fan stall margin modeling accuracy was completed with analysis of in-flight stall tests. Results indicate that the model overestimates the stall margin by between 5 to 10 percent. Because PSC achieves performance gains by using available stall margin, this overestimation may represent performance improvements to be recovered with increased modeling accuracy. Assessment of thrust and stall margin modeling accuracy provides a critical piece for a comprehensive understanding of PSC's capabilities and limitations.

14. SUBJECT TERMS

Airbreathing engines (aircraft); Aircraft engine testing; Aircraft propulsion systems; Engine control systems; Flight tests; Turbofan engines

15. NUMBER OF PAGES

21

16. PRICE CODE

AO3

17. SECURITY CLASSIFICATION OF REPORT	18. SECURITY CLASSIFICATION OF THIS PAGE	19. SECURITY CLASSIFICATION OF ABSTRACT	20. LIMITATION OF ABSTRACT
Unclassified	Unclassified	Unclassified	Unlimited